



## University of Dundee

### Immobilization of elemental mercury by biogenic Se nanoparticles in soils of varying salinity

Wang, Xiaonan; Pan, Xiangliang; Gadd, Geoffrey Michael

*Published in:*  
Science of the Total Environment

*DOI:*  
[10.1016/j.scitotenv.2019.02.457](https://doi.org/10.1016/j.scitotenv.2019.02.457)

*Publication date:*  
2019

*Document Version*  
Peer reviewed version

[Link to publication in Discovery Research Portal](#)

*Citation for published version (APA):*  
Wang, X., Pan, X., & Gadd, G. M. (2019). Immobilization of elemental mercury by biogenic Se nanoparticles in soils of varying salinity. *Science of the Total Environment*, 668, 303-309.  
<https://doi.org/10.1016/j.scitotenv.2019.02.457>

#### General rights

Copyright and moral rights for the publications made accessible in Discovery Research Portal are retained by the authors and/or other copyright owners and it is a condition of accessing publications that users recognise and abide by the legal requirements associated with these rights.

- Users may download and print one copy of any publication from Discovery Research Portal for the purpose of private study or research.
- You may not further distribute the material or use it for any profit-making activity or commercial gain.
- You may freely distribute the URL identifying the publication in the public portal.

#### Take down policy

If you believe that this document breaches copyright please contact us providing details, and we will remove access to the work immediately and investigate your claim.

## **Immobilization of elemental mercury by biogenic Se nanoparticles in soils of varying salinity**

Xiaonan Wang <sup>a,c,d</sup>, Xiangliang Pan <sup>a,b,\*</sup>, Geoffrey Michael Gadd <sup>d</sup>

<sup>a</sup> *Xinjiang Key Laboratory of Environmental Pollution and Bioremediation, Xinjiang Institute of Ecology and Geography, Chinese Academy of Sciences, Urumqi 830011, China*

<sup>b</sup> *College of Environment, Zhejiang University of Technology, Hangzhou 310014, China*

<sup>c</sup> *University of Chinese Academy of Sciences, Beijing 100049, China*

<sup>d</sup> *Geomicrobiology Group, School of Life Sciences, University of Dundee, Dundee DD1 5EH, Scotland, UK*

\*For correspondence. E-mail [panxl@zjut.edu.cn](mailto:panxl@zjut.edu.cn); Tel. +86 571 88320634; Fax +86 571 88320634.

## ABSTRACT

Salinity can be a significant environmental stress which can govern the fate of nanoparticles in the environment as well as other factors such as pH, natural organic matter and minerals. In this research, the effects of salinity on the behaviour of biogenic selenium nanoparticles (BioSeNPs) and consequences for elemental mercury ( $\text{Hg}^0$ ) immobilization in soil and soil solutions were investigated. It was found that homoaggregation and sedimentation of BioSeNPs were enhanced significantly with increasing salinity. Compression of the electric double layers of BioSeNPs at high ionic strengths resulted in attractive van der Waals forces dominating and leading to enhanced aggregation. Moreover, neutralization of the surface negative charge of BioSeNPs by divalent cations and the bridging of BioSeNPs via calcium binding to surface functional groups were also associated with enhanced aggregation. Such enhanced aggregation exerted inhibition of  $\text{Hg}^0$  immobilization in soil solutions/soils of varying salinity. These results indicate that salinity is an important environmental factor governing aggregation of BioSeNPs and therefore influencing the efficiency of  $\text{Hg}^0$  immobilization, and possible remediation treatments, as a consequence.

**Keywords:** selenium nanoparticles; salinity; aggregation; mercury immobilization

## 1. Introduction

Nanoparticles (NPs) are materials having any external dimension in the nanoscale or with an internal/surface structure in the nanoscale (Magdolenova et al., 2014). NPs are receiving huge attention due to their unique properties such as size, surface structure, shape and high reactivity (Shelley, 2005; Farré et al., 2009). Around 40–50% of the atoms in NPs are on the surface, meaning that NPs can have special biological effects unlike their micro- and macro scale counterparts (Auffan et al., 2009). NPs have been widely used in textiles, cosmetics, electronic devices, disease diagnostics and remediation of contaminated environments (Schmid, 2010; Ju-Nam and Lead, 2008). It is known that biogenic selenium nanoparticles (BioSeNPs) have a stronger mercury (Hg) capture capacity (188 mg Hg g<sup>-1</sup>) than chemically synthesised SeNPs or SeNPs at the micro/macro scale (Johnson et al., 2008). Moreover, BioSeNPs have been demonstrated to be an effective bioremediation technique for immobilization of elemental mercury (Hg<sup>0</sup>) in soil and water because of the reaction:  $\text{Hg}^0 + \text{Se}^0 \rightarrow \text{HgSe}$  ( $\Delta G^0 = -38.1 \text{ kJ mol}^{-1}$ ) (Wang et al., 2017; 2018a).

With the increasing development of nanotechnology, large amounts of NPs have been released into the environment and their fate is considered to be an emerging environmental concern. NPs in the environment are subject to a wide range of processes: homoaggregation, adsorption of dissolved organic matter,

complexation by ions, heteroaggregation to particulate matter and subsequent sedimentation, dissolution and chemical transformation. Environmental factors such as salinity, ionic strength, pH, organic matter and clay minerals are the most significant parameters governing the fate of NPs in the environment ([Baalousha et al., 2013](#); [Zhu et al., 2014](#); [Wang et al., 2019](#)).

Salinity is a major environmental stress, and the term refers to the presence of major dissolved inorganic solutes especially  $\text{Na}^+$ ,  $\text{K}^+$ ,  $\text{Mg}^{2+}$ ,  $\text{Ca}^{2+}$ ,  $\text{Cl}^-$ ,  $\text{SO}_4^{2-}$ ,  $\text{HCO}_3^-$  and  $\text{CO}_3^{2-}$  in solution, and is associated with soluble and readily dissolvable salts in soil ([Rhoades, 1996](#)). Salinity can have a significant influence on metal ion speciation. For example, increasing salinity can decrease concentrations of  $\text{Cu}^{2+}$  and  $\text{Zn}^{2+}$  due to precipitation and complexation, and alleviate toxicity ([Park et al., 2014](#)). Research on the role of salinity in determining the bioavailability and toxicity of NPs has received current interest ([Kataoka et al., 2015](#); [Qin et al., 2017](#)). For instance, a reduced electrical double layer (EDL) resulted in an increased hydrodynamic diameter of AgNPs with increasing salinity, and AgNPs were likely to agglomerate to a larger size under high salinity than for low salinity ([Joo et al., 2013](#)). In general, greater salinity can lead to lower toxicity of NPs since lower concentrations of metal ions may be released from metal and metal oxide NPs ([Yung et al., 2017](#)). However, in contrast, the toxicity of polyvinylpyrrolidone-coated AgNPs increased

significantly with increasing salinity although the toxicity of  $\text{Ag}^+$  decreased (Macken et al., 2012). To date, most of the work on the effects of salinity on NPs are carried out in natural seawater, artificial seawater and saline solutions prepared with chemicals such as NaCl and  $\text{CaCl}_2$  (Kim et al., 2015; Yung et al., 2015). Less attention has been paid to soil salinity which has a different composition to seawater. It is known that 6% of the total land area of the world is affected by salt (Munns and Tester, 2008). It is therefore of great importance to understand the impact of salinity on the stability, transport and environmental fate of NPs because of the increasing environmental applications of nanotechnology.

In this work, the effects of salinity on BioSeNPs and consequences for  $\text{Hg}^0$  immobilization were investigated. A soil solution and soil with varying salinity were prepared using natural salt extracted from a saline soil. Homoaggregation of BioSeNPs in a variety of saline solutions was examined using time-resolved dynamic light scattering, sedimentation of BioSeNPs was examined in settling experiments, and the effects of salinity on  $\text{Hg}^0$  immobilization using BioSeNPs in soil and soil solution of differing salinity were assessed by the measurement of residual concentrations of  $\text{Hg}^0$  using a mercury analyzer and determination of mercury speciation.

## 2. Materials and methods

### 2.1 Preparation of saline solution/soil and BioSeNPs

Natural salt was extracted from a saline soil as follows. 1 kg saline soil was collected from the Korla area, Xinjiang, China and mixed with 5 L Milli-Q water using overhead stirrers for 18 h. This process was repeated several times to make sure that the salt in the saline soil was dissolved completely. Afterwards, the soil particles were allowed to settle in Milli-Q water and the supernatant was filtered through filter-paper to obtain a solution containing natural salt. This solution was then heated in an electric furnace to obtain salt through evaporative crystallization. 30% hydrogen peroxide was added to remove organic matter, and the collected salt was finally oven dried. The settled washed desalinated soil was air dried for future use. Reconstituted soil solution/soil of varying salinity (0, 0.2, 1, 3, 5, 10%) was prepared artificially by dissolving appropriate amounts of natural salt in Milli-Q water/air dried settled desalinated soil. Electric conductivity, pH, and concentrations of  $K^+$ ,  $Ca^{2+}$ ,  $Na^+$ ,  $Mg^{2+}$ ,  $Cl^-$  and  $SO_4^{2-}$  were determined as described previously ([Wang et al., 2018a](#)).

Biogenic SeNPs (BioSeNPs) were obtained through the reduction of sodium selenite (1 mM) by *Citrobacter freundii* Y9, with the collected BioSeNPs from culture supernatants being purified according to Cui et al. ([2016](#)) and freeze-dried for future use. Purified BioSeNPs were characterized using transmission

electron microscopy with energy-dispersive X-ray spectrometry (TEM-EDS) (FEI Tecnai G2 F20 S-TWIN, Houston, USA) and X-ray diffraction (XRD) (Bruker D8, Karlsruhe, Germany). A single drop of BioSeNPs solution was dried on a 200-mesh copper TEM grid for TEM-EDS examination. The X-ray diffractometer was equipped with a Cu anode (40 kV and 30 mA) and scanning was from 5 to 80° 2 $\theta$ , and phase identification was carried out as previously described ([Luo et al., 2018](#)).

## *2.2 Zeta potential*

The zeta potential of BioSeNPs (50 mg L<sup>-1</sup>) as a function of pH over the range pH 3-10 in varied saline solutions (0, 0.2, 1, 3, 5, 10% (w/v)) was measured using a Zetasizer Nano ZS90 (Malvern, Worcestershire, UK).

## *2.3 Aggregation*

The homoaggregation of BioSeNPs (50 mg L<sup>-1</sup>) in saline solution (0, 0.2, 1, 3, 5, 10%) was determined by time-resolved dynamic light scattering (DLS) (Malvern Zetasizer Nano ZS90, Worcestershire, UK). Based on the profiles of homoaggregation, the initial aggregation constant (k) was calculated from the increase of D<sub>h</sub>(t) with time (t) as shown in equation 1, and the attachment



efficiency ( $\alpha$ ) obtained by normalizing  $k$  to  $k_{\text{fast}}$  as presented in equation 2 (Schudel et al., 1997; Huynh and Chen, 2011; Huangfu et al., 2013).

$$k \propto \frac{1}{N_0} \left\{ \frac{dD_h(t)}{dt} \right\}_{t \rightarrow 0} \quad (1)$$

$N_0$ : original concentration of BioSeNPs

$D_h(t)$ : the hydrodynamic diameter of BioSeNPs at different times

$$\alpha = \frac{k}{k_{\text{fast}}} = \frac{\frac{1}{N_0} \left\{ \frac{dD_h(t)}{dt} \right\}_{t \rightarrow 0}}{\frac{1}{(N_0)_{\text{fast}}} \left\{ \frac{dD_h(t)}{dt} \right\}_{t \rightarrow 0, \text{fast}}} \quad (2)$$

$k_{\text{fast}}$ : diffusion-limited aggregation rate constant of particles determined under favourable conditions

## 2.4 Settling experiments

Settling experiments for 50 mg L<sup>-1</sup> BioSeNPs were conducted in saline solutions (0, 0.2, 1, 3, 5, 10% (w/v)) according to protocols reported previously (Wang et al., 2018a).

## *2.5 Hg immobilization using BioSeNPs in saline solution/soil*

The immobilization of  $\text{Hg}^0$  using BioSeNPs was carried out in  $\text{Hg}^0$ -contaminated saline solution and saline soil separately. The extracted natural salt was added to  $\text{Hg}^0$ -contaminated Milli-Q water as described by Gai et al. (2016). to provide a  $\text{Hg}^0$ -contaminated solution of varying salinity (0, 0.2, 1, 3, 5, 10% (w/v)). BioSeNPs were added to a final concentration of  $50 \text{ mg L}^{-1}$  to the  $\text{Hg}^0$ -contaminated saline solution and shaken for 6 h after which time the residual  $\text{Hg}^0$  remaining in solution was measured using a Hg analyzer (Lumex RA915+, Saint Petersburg, Russia). The preparation of  $\text{Hg}^0$ -contaminated solution, instrument setup and settings for Hg analysis are described in detail in our previous work (Wang et al., 2018b). Differences in the residual  $\text{Hg}^0$  content remaining in the solution among salinity were tested using one-way ANOVA, and differences and correlations were considered statistically significant if  $p < 0.05$ . The statistical test was performed using SPASS 22.0 (SPSS Inc., USA). The precipitate formed after treated with BioSeNPs in saline solution was collected and analysed using TEM-EDS and XRD.

Liquid mercury was added directly to the air-dried settled desalinated soil, and after that, the appropriate amount of natural salt was added to the soil and fully mixed to prepare saline soil of varying salinity (0, 0.2, 1, 3, 5, 10%) and aged for one month. Mercury immobilization experiments were performed in

centrifuge tubes which contained 10 g Hg<sup>0</sup>-contaminated soil of given salinity. 10 ml Milli-Q water containing 50 mg L<sup>-1</sup> BioSeNPs was added to the tubes which were shaken for one week to immobilize the Hg<sup>0</sup>. A modified sequential extraction procedure, as described in Wang et al. (2017), was used to measure mercury speciation including total mercury, elemental mercury, bioavailable mercury, mercury bound to organic matter and residual mercury in the different saline soils before and after Hg<sup>0</sup> immobilization, according to previous research (Biester and Scholz, 1996; Shi et al., 2005).

### 3. Results

#### 3.1 Saline solution/soil and BioSeNPs

The physico-chemical properties of the saline solution and soil are shown in Tables S1 and S2, respectively. The BioSeNPs synthesized by *Citrobacter freundii* Y9 were amorphous SeNPs (Fig. S1).

#### 3.2 Zeta potential

BioSeNPs carried a negative charge over the pH range 3-11 in the different saline solutions as shown in Fig. 1. BioSeNPs were negatively charged, and this increased with increasing pH in Milli-Q water. It was found that the negative charge of BioSeNPs in a saline solution was lower than that in Milli-Q water. Over the range pH 6-8, the magnitude of negative charge followed the order: BioSeNPs in Milli-Q water ( $\sim -20.2$  mV) > BioSeNPs in solution (0.2% salinity) ( $\sim -11.6$  mV) > BioSeNPs in solution (1% salinity) ( $\sim -7.1$  mV) > BioSeNPs in solution (3% salinity) ( $\sim -5.4$  mV) > BioSeNPs in solution (5% salinity) ( $\sim -4.2$  mV) > BioSeNPs in solution (10% salinity) ( $\sim -3.0$  mV).

{ EMBED Origin50.Graph }

Fig. 1. Zeta potential of BioSeNPs as a function of pH in differing saline solution. Symbols represent: (■) zero salinity; (□) 0.2% salinity; (●) 1% salinity; (○)

3% salinity; (▲) 5% salinity; (△) 10% salinity. Error bars represent the standard deviation (n=3).

### 3.3 Aggregation

Homoaggregation profiles of BioSeNPs in various saline solutions are shown in Fig. 2. The hydrodynamic diameter of BioSeNPs increased over a time period of 1 h, and seemed to increase significantly with greater salinity. The attachment efficiencies ( $\alpha$ ) of BioSeNPs in saline solution, which were calculated based on homoaggregation profiles, significantly increased with increasing salinity (Fig. 3).

{ EMBED Origin50.Graph }

Fig. 2. Homoaggregation profiles of BioSeNPs in solutions of varying salinity. Symbols represent: (■) zero salinity; (●) 0.2% salinity; (▲) 1% salinity; (▼) 3% salinity; (◆) 5% salinity; (★) 10% salinity. Typical results are shown from one of several determinations.

{ EMBED Origin50.Graph }

Fig. 3. Attachment efficiencies of BioSeNPs in various saline solutions. Error bars represent the standard deviation (n = 3)

### 3.4 Settling experiments

The settling of BioSeNPs reached equilibrium over a 16 h time period, and the settling efficiency of the BioSeNPs increased with increasing salinity which was in the order: SeNPs in 10% salinity (~ 44.8%) > SeNPs in 5% salinity (~ 42.0%) > SeNPs in 1% salinity (~ 31.3%) > SeNPs in 3% salinity (~ 30.2%) > SeNPs in 0.2% salinity (~ 25.1%) > SeNPs in Milli-Q water (~ 21.2%) (Fig. 4).

{ EMBED Origin50.Graph }

Fig. 4. Settling of BioSeNPs in different saline solutions.  $C_i$  is the concentration of BioSeNPs detected at specific times;  $C_0$  is the initial concentration of BioSeNPs. The concentration of BioSeNPs was assessed using the OD<sub>260nm</sub> of the suspension. Symbols represent: (■) zero salinity; (□) 0.2% salinity; (●) 1% salinity; (○) 3% salinity; (▲) 5% salinity; (△) 10% salinity. Error bars represent the standard deviation (n = 3).

### 3.5 Hg immobilization using BioSeNPs in saline solution/soil

The effect of salinity on Hg<sup>0</sup> immobilization using BioSeNPs in a soil solution are shown in Fig. 5. The residual content of Hg<sup>0</sup> was 891.9 ng in the control, and the Hg<sup>0</sup> content was significantly reduced to 18.2 ng with a 98.0% removal efficiency in the presence of 50 mg L<sup>-1</sup> BioSeNPs. The residual Hg<sup>0</sup> content in soil solution was significantly changed ( $p < 0.05$ ) and it was found that Hg<sup>0</sup> removal efficiency decreased from 98.0% to 92.7-97.5% under saline conditions. Hg<sup>0</sup> removal was most significantly affected at 0.2% salinity with the

removal performance decreasing from 98.0% to 92.7%. In the soil solution with salinities ranging from 1-10‰, the Hg<sup>0</sup> removal efficiency only slightly declined from 98.0% to 96.4-97.5%. The precipitate that formed in the BioSeNPs treated saline solution was composed mainly of Hg and Se, and the mapping scans of Hg and Se were highly in accordance with their distribution in the precipitate (Fig. S2). XRD analysis further revealed that the precipitate was HgSe (Fig. S3).





{ EMBED Origin50.Graph }

Fig. 5. Residual Hg<sup>0</sup> content in various saline solutions after Hg<sup>0</sup> immobilization using 50 mg L<sup>-1</sup> BioSeNPs. The control was conducted without addition of SeNPs. Symbols represent: ■ control; □ zero salinity; ▨ 0.2% salinity; ▩ 1% salinity; ▤ 3% salinity; ▥ 5% salinity; ▦ 10% salinity. Error bars represent the standard deviation (n=3). Values followed by the same letter do not differ significantly at the 5% level according to one-way ANOVA.

The Hg<sup>0</sup> immobilization efficiency of BioSeNPs in Hg<sup>0</sup>-contaminated soil under saline conditions is shown in Fig. 6. For the control, the total Hg content was 3049.3 ng, and most of the Hg occurred as Hg<sup>0</sup> (2909.3 ng) which accounted for 95.4%. Residual Hg was another important fraction (122.5 ng) accounting for 4.0% of the total Hg. Bioavailable Hg and organic mercury were negligible fractions of the total Hg, and only comprised 0.6% of the total Hg. After addition of 50 mg L<sup>-1</sup> BioSeNPs at zero salinity, the Hg<sup>0</sup> fraction decreased markedly to

12.7%. However, the residual Hg fraction increased to 87.3%. It is interesting that the percentage of  $\text{Hg}^0$  of the total Hg increased from 13.2% to 31.9% and the percentage of residual Hg decreased from 86.7% to 68.0% when the salinity of soil was increased from 0.2% to 10%.

{ EMBED Origin50.Graph }

Fig. 6. The percentage of different fractions of Hg in the various saline soils after treatment with  $50 \text{ mg L}^{-1}$  BioSeNPs. The control was conducted without the addition of BioSeNPs. Symbols represent:  residual Hg;  bioavailable Hg;  organic Hg;  elemental Hg. Error bars represent the standard deviation (n=3).



## 4. Discussion

It has been reported that homoaggregation of nanoparticles in aquatic solution is affected by the chemical properties of the solution such as salinity, ionic strength, pH, and cation valency (French et al., 2009; Loosli et al., 2015; Ellis et al., 2016; Yang et al., 2019). Some research has shown that salinity rather than dissolved organic matter is the dominating factor that governs the stability, and especially the aggregation, of TiO<sub>2</sub> and Ag NPs (Wang et al., 2014). Therefore, it is desirable to understand the role of salinity on the aggregation of BioSeNPs and any consequences for Hg immobilization.

A large amount of research has found that salinity has a great impact on the bioavailability and toxicity of nanoparticles in the environment, and this is highly related to the aggregation properties of the nanoparticles (Kataoka et al., 2015; Qin et al., 2017). For example, the effect of AgNPs on certain aquatic biota was associated with the release of Ag<sup>+</sup> or the uptake of nanoscale particles: suspended nanoparticles are likely to cause more negative effects than agglomerated nanoparticles. It was demonstrated that the presence of electrolytes and high ionic strength in a highly saline solution can lead to an increase in AgNPs hydrodynamic diameter which resulted in AgNPs agglomerating to a larger size. Moreover, the decreased surface area of the aggregated AgNPs also decreased the capacity for releasing Ag<sup>+</sup> from AgNPs surfaces (Griffitt et al.,

2008; Joo et al., 2013). This is similar to our results where homoaggregation of BioSeNPs was enhanced with increasing salinity. One explanation is that the outer shell of the electric double layers (EDLs) of nanoparticles are compressed with increasing salinity, which provides a higher ionic strength, meaning that attractive van der Waals forces dominate and lead to enhanced aggregation (Bian et al., 2011). Several works have found that a colloid concentration decreases dramatically because of aggregation and precipitation with increasing salinity (Stolpe and Hassellöv, 2007). Yung et al. (2017) demonstrated that ZnO nanoparticles formed larger aggregates and released less  $\text{Zn}^{2+}$  in high salinity. Park et al. (2014) demonstrated that aggregation and dissolution of CuO and ZnO nanoparticles was affected by salinity and this played an important role in controlling NPs toxicity to *Tigriopus japonicus*.

The enhanced homoaggregation of BioSeNPs in solutions of high salinity is also related to the presence of divalent cations, e.g.  $\text{Ca}^{2+}$  and  $\text{Mg}^{2+}$ . Zhang et al. (2009) reported that the surface charge of nanoparticles could be neutralized by divalent cations such as  $\text{Ca}^{2+}$  leading to eventual aggregation. Complexation between  $\text{Ca}^{2+}$  and carboxyl groups on the surface of citrate-AgNPs decreased the zeta potential and also enhanced aggregation (Badawy et al., 2010). Our data is in agreement with these findings.  $\text{Ca}^{2+}$  and  $\text{Mg}^{2+}$  increased from 6.57 and 179.22 mg L<sup>-1</sup> to 807.23 and 8432.90 mg L<sup>-1</sup>, respectively, when the salinity increased

from 0.2 to 10%. However, the zeta potential of BioSeNPs decreased from -20.3 to -3.2 mV over the pH range 6-8 when the salinity increased from 0 to 10%. Neutralization by divalent cations decreased electrostatic repulsion resulting in enhanced aggregation. There is a clear relationship between zeta potential and attachment efficiency. Electrostatic repulsion is high and  $\alpha$  is nearly zero at very negative zeta potential values, and electrostatic repulsion is almost zero and  $\alpha$  is nearly unity when the zeta potential is nearly zero. Moreover,  $\text{Ca}^{2+}$  can enhance aggregation by forming calcium-bridges between nanoparticles (Chen and Elimelech, 2007). Calcium readily binds to surface functional groups, such as those present in EPS, and this strong affinity can result in interlinking of polymer chains on the surfaces of BioSeNPs (Chen et al., 2007; Jain et al., 2015). Ranka et al. (2015) also demonstrated that  $\text{Ca}^{2+}$  had an important impact on a polymer coating on nanoparticles, and a stabilizing polyelectrolyte coating would typically fail at high salinities because of dehydration and excessive charge screening.

However, some contrasting research has shown that some kinds of nanoparticles do not readily aggregate under saline conditions. For example, increasing salinity decreased the toxicity of  $\text{Ag}^+$ , although the toxicity of polyvinylpyrrolidone-coated AgNPs increased. This increase in toxicity was most likely to be associated with a combination of the surface properties of nanoparticles and their reactivity within highly saline media (Kim et al., 2015).

The effects of salinity on nanoparticles are therefore not only related to the properties of the solution but also associated with the properties of the nanoparticles. The coatings and functional groups on the surfaces of nanoparticles govern how nanoparticles interact with each other and other components in solution which also play a part in controlling the effects of salinity (Navarro et al., 2008; Scown et al., 2010). Booth et al. (2013) found that polymeric nanoparticles (PNPs) synthesised with a non-ionic stabilising agent (Lutensol AT50) could remain in suspension even at 100% salinity compared with PNPs formed with the ionic stabiliser sodium dodecyl sulphate (SDS). One reason for this is that the absence of ionic groups on the surface of nanoparticles means they cannot be impacted by the saline environment. On the other hand, the effects of salinity on nanoparticles are also related to the hydrophobicity/hydrophilicity of the material, since synthesised and purified PNPs with higher hydrophobicities are likely to aggregate under higher saline conditions.

Nanoparticles undergoing aggregation will settle by gravity especially if the size of the aggregates is greater than 1  $\mu\text{m}$ . According to previous work, sedimentation rates were very high for ZnO, CeO<sub>2</sub> and TiO<sub>2</sub> nanoparticles in seawater of high salinity (Keller et al., 2010). This is in accordance with the results presented here where enhanced aggregation due to a compressed electric

double layer, charge neutralization and calcium-bridging led to a greater settling efficiency.

It is known that the unique properties and high reactivity of nanoparticles results from their huge surface area to volume ratio. Enhanced aggregation and settling significantly reduce the surface area and therefore block the access of nanoparticles to other materials. Amorphous BioSeNPs can be used for Hg immobilization from air and water, and in soil because of their strong Hg<sup>0</sup> capturing capacity (Wang et al., 2017; 2018a, b). Environmental factors such as extracellular polymeric substances and goethite can affect Hg<sup>0</sup> immobilization efficiency (Wang et al., 2018a, b). In the present work, increasing salinity in the solution inhibited Hg<sup>0</sup> immobilization using BioSeNPs, but the inhibitory effect was not significantly enhanced with increasing salinity. One reason may be that the electric double layer could not be compressed further with increasing salinity, so the effects of salinity on Hg<sup>0</sup> immobilization in saline solution were not so obvious (Yung et al., 2015). Nevertheless, Hg<sup>0</sup> immobilization efficiency was significantly suppressed in saline soil, and the proportion of Hg<sup>0</sup> transformed to residual Hg by BioSeNPs significantly decreased with increasing salinity, which may be associated with the heterogeneity and complexity of soil. Another important factor may be associated with reduced Hg<sup>0</sup> immobilization with increasing soil salinity. A range of interactions can occur between dissolved

organic matter (DOM) and nanoparticles in soil, the most important being adsorption (Philippe and Schaumann, 2014). DOM can adsorb to the surface of nanoparticles in spite of any initial coating (Stankus et al., 2011). Divalent and trivalent cations were also demonstrated to enhance adsorption of DOM onto nanoparticles (Schlautman and Morgan, 1994; Janot et al., 2010). Erayhem et al. (2014) found that  $Mg^{2+}$  and  $Ca^{2+}$  promoted adsorption of DOM onto  $TiO_2$  nanoparticles through surface charge screening and cation bridging. Increased ionic strength can also enhance the adsorption of DOM on mineral colloids (Zhou et al., 1994; Feng et al., 2005). Thus, increased ionic strength and concentrations of divalent cations caused by increasing salinity may contribute to the adsorption of DOM on BioSeNPs in soil. Such adsorption of DOM onto BioSeNPs could inhibit  $Hg^0$  access to the surface of BioSeNPs and thus lead to inhibition of  $Hg^0$  immobilization.

## 5. Conclusions

Salinity can play a significant role in governing the environmental fate of BioSeNPs. Compressed electric double layers and dominating van der Waals forces under high ionic strength, charge neutralization due to complexation by divalent cations and calcium-bridges all contribute to enhanced aggregation and sedimentation under saline conditions. On aggregation,  $Hg^0$  immobilization was suppressed because of the decreased surface area and reduced access sites of the

BioSeNPs, and the inhibitory effect was more obvious with increasing salinity in soil rather than in soil solutions.

### **Conflict of interest**

The authors declare no competing financial interest.

### **Acknowledgements**

This work was supported by the National Natural Science Foundation of China (U1503281 and U1403181) and the National Key Research and Development Program of China (2018YFC1802901 and 2018YFC1802902). G. M. Gadd gratefully acknowledges an award (NE/M01090/1) under the National Environmental Research Council (UK) Security of Supply of Mineral Resources Grant Program: Tellurium and Selenium Cycling and Supply (TeASe). G. M. Gadd gratefully acknowledges financial support of the Geomicrobiology Group by NERC [NE/M011275/1: (CoG<sup>3</sup>)]. We also acknowledge financial support from the China Scholarship Council and the British Council through the UK-China Joint Research and Innovation Partnership Fund PhD Placement Programme to X. Wang (No. 201703780058).

## References

- Auffan, M., Rose, J., Bottero, J.Y., Lowry, G.V., Jolivet, J.P., Wiesner, M.R., 2009. Towards a definition of inorganic nanoparticles from an environmental, health and safety perspective, *Nat. Nanotechnol.*, 4, 634.
- Baalousha, M., Nur, Y., Römer, I., Tejamaya, M., Lead, J.R., 2013. Effect of monovalent and divalent cations, anions and fulvic acid on aggregation of citrate-coated silver nanoparticles. *Sci. Total Environ.*, 454, 119-131.
- Badawy, A.M.E., Luxton, T.P., Silva, R.G., Scheckel, K.G., Suidan, M.T., Tolaymat, T.M., 2010. Impact of environmental conditions (pH, ionic strength, and electrolyte type) on the surface charge and aggregation of silver nanoparticles suspensions, *Environ. Sci. Technol.*, 44, 1260-1266.
- Bian, S.W., Mudunkotuwa, I.A., Rupasinghe, T., Grassian, V.H., 2011. Aggregation and dissolution of 4 nm ZnO nanoparticles in aqueous environments: influence of pH, ionic strength, size, and adsorption of humic acid, *Langmuir*, 27, 6059–6068.
- Biester, H., Scholz, C., 1996. Determination of mercury binding forms in contaminated soils: mercury pyrolysis versus sequential extractions, *Environ. Sci. Technol.*, 31, 233-239.
- Booth, A.M., Justynska, J., Kubowicz, S., Johnsen, H., Frenzel, M., 2013. Influence of salinity, dissolved organic carbon and particle chemistry on the



aggregation behaviour of methacrylate-based polymeric nanoparticles in aqueous environments, *Int. J. Environ. Pollut.*, 52, 15-31.

Chen, K.L., Elimelech, M., 2007. Influence of humic acid on the aggregation kinetics of fullerene (C60) nanoparticles in monovalent and divalent electrolyte solutions, *J. Colloid Interface Sci.*, 309, 126-134.

Chen, K.L., Mylon, S.E., Elimelech, M., 2007. Enhanced aggregation of alginate-coated iron oxide (hematite) nanoparticles in the presence of calcium, strontium, and barium cations, *Langmuir*, 23, 5920-5928.

Cui, Y., Li, L., Zhou, N., Liu, J., Huang, Q., Wang, H., Tian, J., Yu, H., 2016. In vivo synthesis of nano-selenium by *Tetrahymena thermophila* SB210, *Enzyme Microb. Technol.*, 95, 185-191.

Ellis, L.J.A., Valsami-Jones, E., Lead, J.R., Baalousha, M., 2016. Impact of surface coating and environmental conditions on the fate and transport of silver nanoparticles in the aquatic environment. *Sci. Total Environ.*, 568, 95-106.

Erhayem, M., Sohn, M., 2014. Stability studies for titanium dioxide nanoparticles upon adsorption of Suwannee River humic and fulvic acids and natural organic matter. *Sci. Total Environ.*, 468, 249–257.

Farré, M., Gajda-Schrantz, K., Kantiani, L., Barceló, D., 2009. Ecotoxicity and analysis of nanomaterials in the aquatic environment, *Anal. Bioanal. Chem.*, 393, 81–95.

Feng, X., Simpson, A.J., Simpson, M.J., 2005. Chemical and mineralogical controls on humic acid sorption to clay mineral surfaces. *Org. Geochem.*, 36, 1553–1566.

French, R.A., Jacobson, A.R., Kim, B., Isley, S.L., Penn, R.L., Baveye, P.C., 2009. Influence of ionic strength, pH, and cation valence on aggregation kinetics of titanium dioxide nanoparticles, *Environ. Sci. Technol.*, 43, 1354–1359.

Gai, K., Hoelen, T.P., Hsu-Kim, H., Lowry, G.V., 2016. Mobility of four common mercury species in model and natural unsaturated soils, *Environ. Sci. Technol.*, 50, 3342–3351.

Griffitt, R.J., Luo, J., Gao, J., Bonzongo, J.C., Barber, D.S., 2008. Effects of particle composition and species on toxicity of metallic nanomaterials in aquatic organisms, *Environ. Toxicol. Chem.*, 27, 1972–1978.

Huangfu, X., Jiang, J., Ma, J., Liu, Y., Yang, J., 2013. Aggregation kinetics of manganese dioxide colloids in aqueous solution: influence of humic substances and biomacromolecules, *Environ. Sci. Technol.*, 47, 10285–10292.

Huynh, K.A., Chen, K.L., 2011. Aggregation kinetics of citrate and polyvinylpyrrolidone coated silver nanoparticles in monovalent and divalent electrolyte solutions, *Environ. Sci. Technol.*, 45, 5564–5571.

Jain, R., Jordan, N., Weiss, S., Foerstendorf, H., Heim, K., Kacker, R., Hübner, R., Kramer, H., Van Hullebusch, E.D., Farges, F., Lens, P.N.L., 2015.

Extracellular polymeric substances govern the surface charge of biogenic elemental selenium nanoparticles, *Environ. Sci. Technol.*, 49, 1713–1720.

Janot, N., Benedetti, M.F., Reiller, P.E., 2010. Colloidal  $\alpha\text{-Al}_2\text{O}_3$ , europium (III) and humic substances interactions: a macroscopic and spectroscopic study. *Environ. Sci. Technol.*, 45, 3224–3230.

Johnson, N.C., Manchester, S., Sarin, L., Gao, Y., Kulaots, I., Hurt, R.H., 2008. Mercury vapor release from broken compact fluorescent lamps and in situ capture by new nanomaterial sorbents, *Environ. Sci. Technol.*, 42, 5772-5778.

Joo, H.S., Kalbassi, M.R., Yu, I.J., Lee, J.H., Johari, S.A., 2013. Bioaccumulation of silver nanoparticles in rainbow trout (*Oncorhynchus mykiss*): influence of concentration and salinity, *Aquat. Toxicol.*, 140, 398-406.

Ju-Nam, Y., Lead, J.R., 2008. Manufactured nanoparticles: an overview of their chemistry, interactions and potential environmental implications. *Sci. Total Environ.*, 400, 396-414.

Kataoka, C., Ariyoshi, T., Kawaguchi, H., Nagasaka, S., Kashiwada, S., 2015. Salinity increases the toxicity of silver nanocolloids to Japanese medaka embryos, *Environ. Sci. Nano*, 2, 94-103.

Keller, A.A., Wang, H., Zhou, D., Lenihan, H.S., Cherr, G., Cardinale, B.J., Miller, R., Ji, Z., 2010. Stability and aggregation of metal oxide nanoparticles in natural aqueous matrices, *Environ. Sci. Technol.*, 44, 1962-1967.

Kim, I., Taghavy, A., DiCarlo, D., Huh, C., 2015. Aggregation of silica nanoparticles and its impact on particle mobility under high-salinity conditions, J. Pet. Sci. Eng., 133, 376-383.

Loosli, F., Le Coustumer, P., Stoll, S., 2015. Effect of electrolyte valency, alginate concentration and pH on engineered TiO<sub>2</sub> nanoparticle stability in aqueous solution. Sci. Total Environ., 535, 28-34.

Luo, H., Law, W.W., Wu, Y., Zhu, W., Yang, E.H., 2018. Hydrothermal synthesis of needle-like nanocrystalline zeolites from metakaolin and their applications for efficient removal of organic pollutants and heavy metals. Microporous Mesoporous Mater., 272, 8-15.

Macken, A., Byrne, H.J., Thomas, K.V., 2012. Effects of salinity on the toxicity of ionic silver and Ag-PVP nanoparticles to *Tisbe battagliai* and *Ceramecium tenuicorne*, Ecotoxicol. Environ. Saf., 86, 101-110.

Magdolenova, Z., Collins, A., Kumar, A., Dhawan, A., Stone, V., Dusinska, M., 2014. A review of in vitro and in vivo studies with engineered nanoparticles, Nanotoxicology, 8, 233-278.

Munns, R., Tester, M., 2008. Mechanisms of salinity tolerance, Annu. Rev. Plant Biol., 59, 651-681.

Navarro, E., Baun, A., Behra, R., Hartmann, N.B., Filser, J., Miao, A.J., Quigg, A., Santschi, P.H., Sigg, L., 2008. Environmental behavior and ecotoxicity of engineered nanoparticles to algae, plants, and fungi, *Ecotoxicology*, 17, 372–386.

Park, J., Kim, S., Yoo, J., Lee, J.S., Park, J.W., Jung, J., 2014. Effect of salinity on acute copper and zinc toxicity to *Tigriopus japonicus*: the difference between metal ions and nanoparticles, *Mar. Pollut. Bull.*, 85, 526-531.

Philippe, A., Schaumann, G.E., 2014. Evaluation of hydrodynamic chromatography coupled with UV-visible, fluorescence and inductively coupled plasma mass spectrometry detectors for sizing and quantifying colloids in environmental media. *PLoS One*, 9, e90559.

Qin, Y., Guo, X., Tou, F., Pan, H., Feng, J., Xu, J., Chen, B., Liu, M., Yang, Y., 2017. Cytotoxicity of TiO<sub>2</sub> nanoparticles toward *Escherichia coli* in an aquatic environment: effects of nanoparticle structural oxygen deficiency and aqueous salinity, *Environ. Sci. Nano*, 4, 1178-1188.

Ranka, M., Brown, P., Hatton, T.A., 2015. Responsive stabilization of nanoparticles for extreme salinity and high-temperature reservoir applications, *ACS Appl. Mater. Interfaces*, 7, 19651-19658.

Rhoades, J.D., 1996. Salinity: electrical conductivity and total dissolved solids. In: Sparks, D.L., (Ed.), *Methods of Soil Analysis Part 3—Chemical Methods*, Soil Science Society of America, Madison, pp. 417-435.

Schlautman, M.A., Morgan, J.J., 1994. Adsorption of aquatic humic substances on colloidal-size aluminum oxide particles: influence of solution chemistry. *Geochim. Cosmochim. Acta*, 58, 4293–4303.

Schmid, G., 2010. *Nanoparticles: From Theory to Application*, Second ed. Wiley VCH, Weinheim.

Schudel, M., Behrens, S.H., Holthoff, H., Kretzschmar, R., Borkovec, M., 1997. Absolute aggregation rate constants of hematite particles in aqueous suspensions: a comparison of two different surface morphologies, *J. Colloid Interface Sci.*, 196, 241–253.

Scown, T.M., Van Aerle, R., Tyler, C.R., 2010. Do engineered nanoparticles pose a significant threat to the aquatic environment? *Crit. Rev. Toxicol.*, 40, 7, 653–670.

Shelley, S.A., 2005. Nanotechnology: turning basic science into reality. In: Theodore, L., Kunz, R.G., (Ed.), *Nanotechnology: Environmental Implications and Solutions*, John Wiley & Sons, Hoboken.

Shi, J., Liang, L., Jiang, G., Jin, X., 2005. The speciation and bioavailability of mercury in sediments of Haihe River, China, *Environ. Int.*, 31, 357-365.

Stankus, D.P., Lohse, S.E., Hutchison, J.E., Nason, J.A., 2011. Interactions between natural organic matter and gold nanoparticles stabilized with different organic capping agents. *Environ. Sci. Technol.*, 45, 3238–3244.

Stolpe, B., Hassellöv, M., 2007. Changes in size distribution of fresh water nanoscale colloidal matter and associated elements on mixing with seawater, *Geochim. Cosmochim. Acta*, 71, 3292–3301.

Wang, H., Burgess, R.M., Cantwell, M.G., Portis, L.M., Perron, M.M., Wu, F., Ho, K.T., 2014. Stability and aggregation of silver and titanium dioxide nanoparticles in seawater: role of salinity and dissolved organic carbon, *Environ. Toxicol. Chem.*, 33, 1023-1029.

Wang, X., Pan, X., Gadd, G.M., 2019. Soil dissolved organic matter affects mercury immobilization by biogenic selenium nanoparticles. *Sci. Total Environ.*, 658, 8-15.

Wang, X., Song, W., Qian, H., Zhang, D., Pan, X., Gadd, G.M., 2018a. Stabilizing interaction of exopolymers with nano-Se and impact on mercury immobilization in soil and groundwater, *Environ. Sci. Nano*, 5, 456-466.

Wang, X., Zhang, D., Pan, X., Lee, D.J., Al-Misned, F.A., Golam Mortuza, M., Gadd, G.M., 2017. Aerobic and anaerobic biosynthesis of nano-selenium for remediation of mercury contaminated soil, *Chemosphere*, 170, 266–273.

Wang, X., Zhang, D., Qian, H., Liang, Y., Pan, X., Gadd, G.M., 2018b. Interactions between biogenic selenium nanoparticles and goethite colloids and consequence for remediation of elemental mercury contaminated groundwater, *Sci. Total Environ.*, 613, 672-678.

Yang, W., Shang, J., Sharma, P., Li, B., Liu, K., Flury, M., 2019. Colloidal stability and aggregation kinetics of biochar colloids: Effects of pyrolysis temperature, cation type, and humic acid concentrations. *Sci. Total Environ.* 658, 1306-1315.

Yung, M.M., Kwok, K.W., Djurišić, A.B., Giesy, J.P., Leung, K.M., 2017. Influences of temperature and salinity on physicochemical properties and toxicity of zinc oxide nanoparticles to the marine diatom *Thalassiosira pseudonana*, *Sci. Rep.*, 7, 3662.

Yung, M.M., Wong, S.W., Kwok, K.W., Liu, F.Z., Leung, Y.H., Chan, W.T., Li, X.Y., Djurišić, A.B., Leung, K.M., 2015. Salinity-dependent toxicities of zinc oxide nanoparticles to the marine diatom *Thalassiosira pseudonana*, *Aquat. Toxicol.*, 165, 31-40.

Zhang, Y., Chen, Y., Westerhoff, P., Crittenden, J., 2009. Impact of natural organic matter and divalent cations on the stability of aqueous nanoparticles, *Water Res.*, 43, 4249-4257.

Zhou, J.L., Rowland, S., Fauzi, R., Mantoura, C., Braven, J., 1994. The formation of humic coatings on mineral particles under simulated estuarine conditions-a mechanistic study. *Water Res.*, 28, 571–579.



Zhu, M., Wang, H., Keller, A.A, Wang, T., Li, F., 2014. The effect of humic acid on the aggregation of titanium dioxide nanoparticles under different pH and ionic strengths. *Sci. Total Environ.*, 487, 375-380.